

EXPERIMENTAL INVESTIGATION TO IMPROVE THE PERFORMANCE OF THE PV MODULE USING GRAPHENE HYDROPHOBIC NANO COATING COUPLED WITH TOP WATER COOLING

by

Karthik MYILSWAMY^{a*} and Kannan KUMARESAN^b

^aDepartment of Mechanical Engineering, Sri Shakthi Institute of Engineering and Technology, Coimbatore, India

^bDepartment of Mechanical Engineering, PSG College of Technology, Coimbatore, India

Original scientific paper
<https://doi.org/10.2298/TSCI240803008M>

This research aims to enhance the efficiency of polycrystalline silicon solar photovoltaic panels by addressing the dual challenges of dust accumulation and temperature variations. The study investigates the effects of applying a hydrophobic graphene nanocoating on the top surface of the panels to prevent dust buildup, coupled with a top water-cooling system to regulate panel temperature. Outdoor experiments were conducted in Coimbatore, India, from 8:00 a. m. to 4:00 p. m. under sunny conditions for 40 days. A total of eight identical photovoltaic panels were tested with various configurations, and performance parameters such as glass temperature, Tedlar® temperature, output power, solar radiation, ambient temperature, and wind speed were recorded. Experimental results show that the graphene nanocoating reduces panel temperature by 9.36% compared to the dusty panel and 3.8% compared to the uncoated, manually cleaned panel by day 40. The nanocoating alone increased power output and efficiency by 4.16% and 3.3%, respectively, compared to the uncoated, no-cooling panel. Additionally, the nano-coated, top water-cooled panels showed improvements of 16.87% in output power and 13.22% in efficiency compared to the uncoated, no-cooling panel, and 3.11% in power and 2.82% in efficiency compared to the uncoated, water-cooled panels. These results demonstrate that the combined application of graphene nanocoating and water cooling effectively enhances the performance and longevity of photovoltaic modules by reducing dust accumulation and regulating temperature.

Key words: photovoltaic performance, dust deposition, nanocoating, top water cooling

Introduction

Solar energy is widely recognized as a clean and RES, garnering significant scientific interest worldwide. Among the various solar technologies, photovoltaic (PV) systems hold a prominent position due to their capability to efficiently convert solar radiation into electrical energy via the photoelectric effect, as highlighted by Ilse *et al.* [1]. The efficiency of PV modules is strongly influenced by their anti-soiling characteristics, as reported by Piliouguine *et al.*

*Corresponding author, e-mail: karthiktist@gmail.com

[2]. Dust accumulation poses a significant challenge, particularly in arid regions where dust storms are prevalent, and rainfall is scarce. This accumulation can severely impact the efficiency of PV panels, as noted by Zhang *et al.* [3]. Excessive dust buildup obstructs PV cells from receiving solar radiation, leading to substantial power generation losses [4]. To address these challenges, researchers have explored various cooling and dust mitigation strategies to enhance PV performance. Innovative cooling methods have been developed to mitigate heat accumulation in PV systems. Abdo and Hind [5] demonstrated that Al_2O_3 -water-based nanofluids coated on PV panels could reduce temperatures by $17.9\text{ }^\circ\text{C}$ and $16.3\text{ }^\circ\text{C}$ at radiation intensities of 800 W/m^2 and 1000 W/m^2 , respectively. Additionally, Almuwailhi and Zeitoun [6] investigated evaporative cooling methods. Their study revealed that natural convection cooling using wetted fabric increased daily energy production by 1.7% and efficiency by 1.2%, while forced convection cooling with air at a velocity of 3 m/s improved energy production and efficiency by 4.4% and 4%, respectively.

Sethiya [7] proposed glycerol as a cooling agent to maintain PV cells at a standard temperature of $25\text{ }^\circ\text{C}$. Similarly, Elbreki *et al.* [8] conducted experiments using passive fin heat sinks, reporting a reduction of $24.6\text{ }^\circ\text{C}$ in PV module temperature, which increased electrical efficiency by 10.68% and power output by 37.1 W under real environmental conditions. Furthermore, Al-Amri *et al.* [9] compared heat sink-based and PCM heat sink configurations, concluding that heat sinks provided superior cooling with a temperature drop of $10\text{ }^\circ\text{C}$. Dust deposition significantly reduces the efficiency of PV panels. Sharma and Chandel [10] reported a 70% drop in efficiency for uncleaned systems compared to routinely cleaned ones, emphasizing the critical impact of dust. He *et al.* [11] highlighted that manual cleaning methods, although effective, are resource intensive and may result in secondary environmental pollution. In contrast, Moghimi and Ahmadi [12] pointed out that natural phenomena, such as rain and wind, provide eco-friendly mechanisms for dust removal. Advanced coatings have also been explored to mitigate dust accumulation. Elnozahy *et al.* [13] examined hydrophilic nanocoatings, which increased module output power by 18% compared to manually cleaned panels.

Zhang *et al.* [14] demonstrated that ethanol solution with SiO_2 nanocoatings on glass surfaces minimized power efficiency losses and enhanced spectral transmittance. Fares and Yusuf [15] analyzed anti-soiling coatings for GaAs and c-Si PV cells, finding improved energy and exergy efficiencies after two weeks of exposure. Vedula and Geetha [16] studied the impact of various dust particles under controlled conditions, revealing power output reductions for materials like cement (0.067%), fly ash (0.164%), and coal (0.177%). Bazzari *et al.* [17] investigated ZnO nanoparticles as luminescent down-shifting materials, reporting a $4.5\text{ }^\circ\text{C}$ reduction in PV cell temperature. Zhang *et al.* [18] explored hydrophobic coatings, noting substantial reductions in dust deposition density based on surface inclination angles. Jaszczur *et al.* [19] analyzed the correlation between PV panel temperature and dust adhesion, reporting a 480.0 mg dust accumulation over one week, resulting in a 2.1% efficiency drop. Such findings underscore the importance of addressing dust-related challenges to optimize PV performance and ensure sustainable energy production. This comprehensive literature review indicates that hydrophobic coatings and water-based cooling methods offer promising approaches for improving the performance of PV systems. However, their combined and individual effects, particularly under diverse environmental and operational conditions, have not been thoroughly investigated.

To address these gaps, the present research aims to improve the performance of polycrystalline silicon solar PV panels by mitigating the adverse effects of both temperature fluctuations and dust accumulation. A hydrophobic graphene nanocoating will be applied to minimize

dust deposition, while a top water-cooling system will be implemented to effectively manage panel temperature. The study will involve extensive outdoor experiments to evaluate the individual and combined impacts of these techniques on the power output and efficiency of the PV panels. Data collected under real-world conditions will offer critical insights for enhancing the overall performance and reliability of solar PV systems.

Materials and methods

Nanocoating and top water-cooling method

The nanocoating applied to the solar PV panels forms a transparent protective film that prevents the accumulation of dust particles on the surface. In this study, a commercially available graphene-based nanocoating material [20] was used. This material offers high transmittance (approximately 90%) and low reflectance (2%-5%), which enhances sunlight absorption and improves overall energy efficiency. Its hydrophobic properties, with a contact angle greater than 100°, effectively reduce dust buildup and promote self-cleaning, minimizing maintenance needs.

For this experiment, 103.1 ml/m² of coating was applied for a single layer, and 226.8 ml/m² for three layers. The thickness of the nanocoating was 112.5 microns for a single layer and 247.7 microns for three layers. Prior to application, the top surface of the PV panels was thoroughly cleaned, dried, and inspected to ensure it was free from oil, fingerprints, or detergent residue. The nanocoating was applied in circular motions using a microfiber cloth, followed by a 60 minute air drying process. In high-humidity conditions, drying time was extended to ensure optimal results. Once applied, the panel surface exhibited a slightly rough texture, preventing water from settling, and displayed a rainbow-like effect when viewed at an angle. For the water-cooling system, a circular PVC pipe, 3 mm in diameter with 110 evenly spaced holes, was placed over the PV panel to introduce a water layer. The water flow rate was regulated using a valve positioned between the inlet tube and the water tank, ensuring precise control over the flow.

Experimental methodology

The experimental set-up for the evaluation of solar PV panels with various cooling and nano coating techniques was designed to ensure accurate data collection and analysis. A polycrystalline silicon PV module was securely mounted on a rigid steel frame to maintain system stability and facilitate easy adjustment of the inclination angle.

The outdoor experiment took place in Coimbatore, India, where the climate conditions were conducive for solar energy generation. The testing period spanned from 8.00 a. m. to 4.00 p. m. on sunny days, with the PV module positioned at an optimal slope of 13° facing South. In this study, eight identical PV panels were utilized, each subjected to different treatments. The first panel served as the reference panel, remaining uncoated and without any cooling mechanism. The second panel was cooled using water on the top side, while the third panel had a graphene nanomaterial coating applied to the top side. The fourth panel benefited from both graphene nanocoating and water cooling on the top side. The experiment involved using four clean panels on the first day, followed by a combination of four cleaned panels and four naturally dusted panels from the second day onwards. Over a period of 40 days, all eight experiments were conducted simultaneously, with data on PV characteristics, output power, solar radiation, ambient temperature, and efficiency of the solar PV panels scrupulously recorded. The experimental setup, as depicted in fig. 1, allowed for precise monitoring and data collection. Throughout the 40 day duration, readings of voltage, current, ambient temperature, and solar

irradiation were logged every 15 seconds for all types of panels. The flowchart for the experimental methodology as shown in fig. 2.



Figure 1. Experimental set-up of the present research

Devices, instruments and measurements

In the experiment, eight identical polycrystalline PV modules, each with a nominal peak power of 165 W, were used. The detailed specifications of the solar PV modules, as provided in the manufacturer's data sheet, are summarized in tab. 1. A PWM 12 V, 50 A MPPT solar charge controller was employed for efficient battery charging and for regulating the solar panel output. This advanced controller ensured optimal charging efficiency while protecting the battery from overcharging and over-discharging. The energy generated by the PV panels was stored in an exide power save Plus-12 V sealed lead acid battery. Experimental data were meticulously recorded using an Arduino Mega 2560

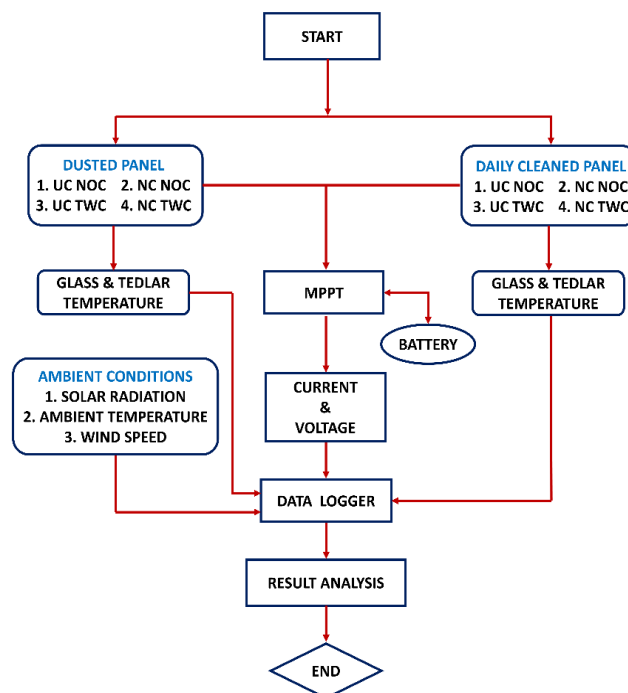


Figure 2. Flow chart for methodology

data logger, which captured critical parameters such as solar radiation, wind speed, ambient temperature, panel temperature, water inlet and outlet temperatures, output current, and voltage. Temperature measurements were conducted using *K*-type thermocouples, while solar irradiation was measured with a DBTU1300 solarimeter. Current and voltage outputs were precisely measured using a WCS1700 current sensor module and a voltage sensor module (0-25 V range), respectively. Additionally, an anemometer was employed to measure wind speed.

Table 1. Solar PV module geometrical and technical values

Name	Value
Module size	1480 × 670 × 34 ±2 [mm]
Cell type	Polycrystalline
Number of cells	36
Maximum power, P_{mp}	165 [W]
Maximum power current, I_{mp}	8.85 [A]
Maximum power voltage, V_{mp}	18.65 [V]
Short circuit current, I_{sc}	9.55 [A]
Open circuit voltage, V_{oc}	22.84 [V]

This study explored the performance of solar PV systems under outdoor environmental conditions, focusing on cooling techniques, nanocoating applications, and the use of advanced measuring instruments for data acquisition. Through systematic experimentation and comprehensive data collection, valuable insights were gained into the efficiency and operational dynamics of the photovoltaic modules.

Uncertainty analysis

The methodology described was employed to estimate the experimental uncertainty associated with this study. The individual uncertainties of the measured variables were calculated and are summarized in tab. 2. The analysis indicates that the measuring instruments used in the experiments demonstrate an acceptable level of geometric uncertainty. Therefore, it can be concluded that the influence of measurement errors on the overall results is negligible.

Table 2. Uncertainty analysis

Sl.No	Measurement	Uncertainty [%]
1	Thermocouple type K	±0.88
2	Flowmeter	±0.87
3	Solar radiation intensity	±0.6
4	Voltage	±0.5
5	Current	±0.73

The equation for the overall uncertainty, U , of the experiment was calculated using the root-sum-square method, as [21]:

$$U = \left(\sum_{i=1}^n \left(\frac{\delta R}{\delta x_i} \mu_i \right)^2 \right)^{1/2} \quad (1)$$

where R is the result derived from the measurements, while x_i denotes the measured variables. The term $\delta R/\delta x_i$ is the sensitivity coefficient, which indicates how R changes with respect to each variable x_i . The value μ_i represents the uncertainty in the measurement of x_i and n is the total number of variables involved in the experiment.

The PV output power and efficiency calculation

Based on the experimental data, the output power and electrical efficiency of the PV module are calculated using the appropriate theoretical formulas. The maximum electrical power of a PV system can be expressed as:

$$P_{\max} = V_{\text{mp}} I_{\text{mp}} \quad (2)$$

where V_{mp} [V] is the maximum peak voltage, I_{mp} [A] – the maximum peak current, and P_{mp} [W] – the maximum peak power of the PV panel.

The performance of the solar panel is often evaluated in terms of its electrical efficiency, which is determined by the ratio of the maximum power output to the solar radiation incident on the surface of the panel. The electrical efficiency, η_{ele} is given by:

$$\eta_{\text{ele}} = \frac{P_{\max}}{GA} \quad (3)$$

where G [Wm^{-2}] is the solar irradiance and A [m^2] – the surface area of the PV panel.

Results and discussion

Figure 3 illustrates the hourly measurements of solar radiation at the specific location where the study was carried out during the experimental period. The data gathered revealed that the daily solar radiation levels at the site ranged from 7.23-7.78 kWh/m^2 . This significant range indicates a substantial potential for solar energy utilization at the experimental site, particularly for the installation of PV systems. Furthermore, it was observed that there was minimal daily variation in solar radiation throughout the 40 day duration of the experimental study.

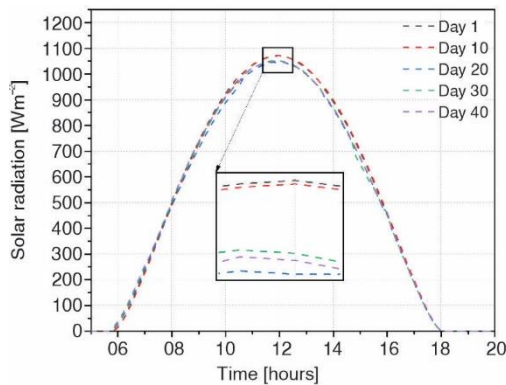


Figure 3. Hourly solar radiation in W/m^2 of different days of the site under study

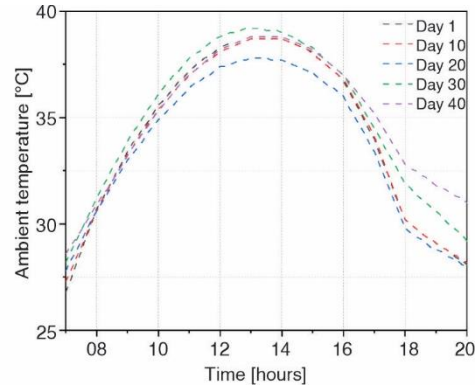


Figure 4. Hourly ambient temperature in $^{\circ}\text{C}$ of different days of the site under study

The hourly ambient temperatures recorded during the experimental period are presented in fig. 4. The data reveals that the average ambient temperature remained around 33 $^{\circ}\text{C}$ over the course of the study. The maximum ambient temperature varied between 37.8 $^{\circ}\text{C}$ and 39.2 $^{\circ}\text{C}$, with day 30 recording the highest value of 39.2 $^{\circ}\text{C}$. These fluctuations in ambient temperature have a significant effect on the temperature of the PV panels. As the ambient temperature rises, the panel temperature increases, leading to a reduction in their efficiency. This temperature-dependent performance decrease is a well-established phenomenon, as higher temperatures can negatively impact the electrical output of solar panels by increasing resistive

losses and reducing the voltage output. The recorded minimum temperature of 22 °C was observed on day 1, and it gradually increased over the following days, indicating the influence of seasonal variations on the outdoor environment. The rise in temperature during the experiment underscores the importance of considering temperature management strategies, such as cooling techniques and nanocoating applications, to enhance the performance of solar panels.

Figure 5 illustrates the wind speed measurements taken on various days at the site under investigation. The data indicates that the wind speed reached its peak during the afternoon hours, while it was at its lowest in the morning and evening. Throughout the experimental period, the maximum recorded wind speed was 3.2 m/s, whereas the minimum was 0.3 m/s. This variation in wind speed plays a crucial role in enhancing the convection heat transfer between the top and bottom sides of the solar panel to the surrounding environment. As a result, this increased heat transfer leads to a decrease in the temperature of the solar panel. The average wind speed in Tamil Nadu at a height of 3 m to 4 m above ground level can vary depending on the specific location and time of year. However, based on general trends and data, it's typically in the range of 3 m/s to 5 m/s [22].

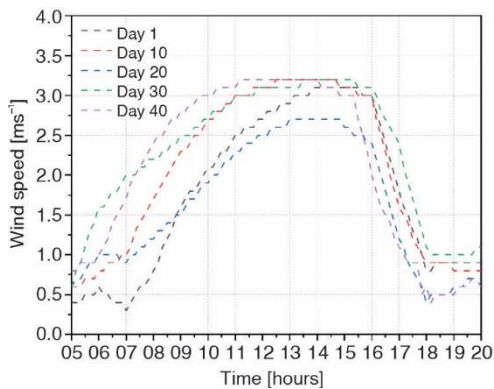


Figure 5. Hourly wind speed in m/s of different days of the site under study

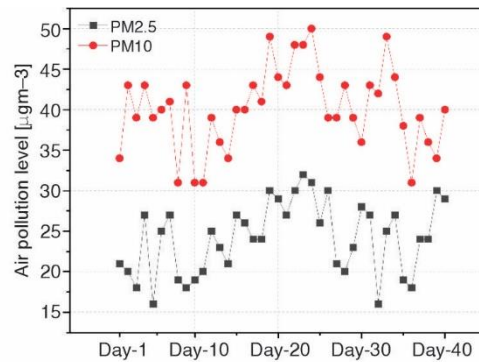


Figure 6. The PM2.5 and PM10 dust concentrations at the experimental site

The influence of dust deposition on solar panels is of paramount importance, as it significantly impacts their efficiency. The composition of dust can vary depending on the location, resulting in varying levels of efficiency reduction in photovoltaic modules across different regions. The PM2.5 and PM10 concentrations at the experimental conducting site during the designated experimental periods were precisely gathered from the local meteorological department and are visually represented in fig. 6. The average dust deposition on the experimental site for PM2.5 and PM10 was quantified at 24.15 $\mu\text{g}/\text{m}^3$ and 39.15 $\mu\text{g}/\text{m}^3$, respectively. The presence of dust on solar panels can lead to a decrease in their performance due to reduced solar radiation transmission. This can result in a decrease in the overall energy output of the system. Additionally, the accumulation of dust on the surface of solar panels can lead to an increase in temperature, which can further impact the efficiency of the panels.

Figure 7 illustrates the glass temperature of a PV module on day 1 for various configurations, including UC-NOC, NC-NOC, UC-TWC, and NC-TWC. The results showing the maximum glass temperature of the PV module on day 1 reveal 69.52 °C for UC-NOC, 70.12 °C for NC-NOC, 42.46 °C for UC-TWC, and 42.37 °C for NC-TWC, respectively. Also, the nano-coated no-cooling solar PV module can increase the module temperature by about 0.55 °C (0.93%) compared to the un-coated no-cooling panel. In contrast, the NC-TWC PV panel can

decrease the module temperature by about 20.34 °C (33%) and 0.08 °C (0.2%) compared to UC-NOC and UC-TWC. On day 1, when compared with the UC-NOC module, the NC-NOC module experienced an increase in glass temperature, but at the same time, the NC-TWC module decreased the glass temperature when compared with the UC-TWC.

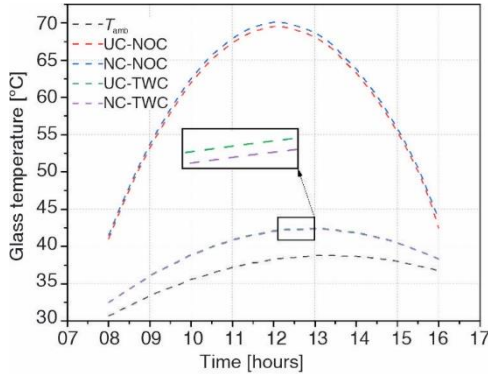


Figure 7. Glass temperature for day 1

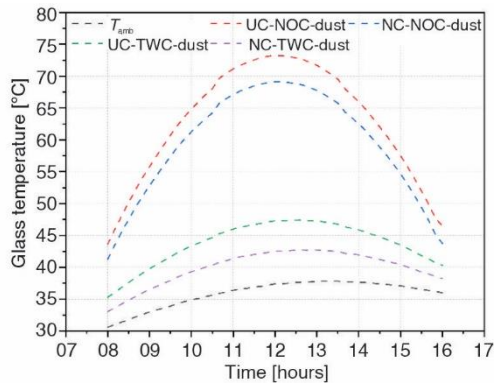


Figure 8. Glass temperature for day 20

Figure 8 presents the PV module glass temperature of an experimental investigation conducted on day 20 for the various configurations of dusted module. The UC-NOC, NC-NOC, UC-TWC, and NC-TWC dusted panels attain the maximum glass temperatures of 73.23 °C, 69.13 °C, 47.40 °C, and 42.74 °C on day 20, respectively. Using graphene nanocoat over a no-cooling solar PV module can decrease the module temperature by about 3.41 °C (5.4%) compared to a UC-NOC panel. Also, the NC-TWC PV panel can decrease the module temperature by about 23.0 °C (35.66%) and 3.79 °C (8.57%) compared to UC-NOC and UC-TWC. Furthermore, the nanocoating over a PV module surface has a positive impact on the cooling of the solar PV module and decreases the panel temperature beyond day 1 for the NC-NOC PV module. Figure 9 presents the PV module glass temperature of an experimental investigation conducted on day 40 for the various configurations of the dusted module. The UC-NOC, NC-NOC, UC-TWC, and NC-TWC dusted panels attain the maximum glass temperatures of 77.88 °C, 70.31 °C, 49.43 °C and 43.98 °C on day 40, respectively.

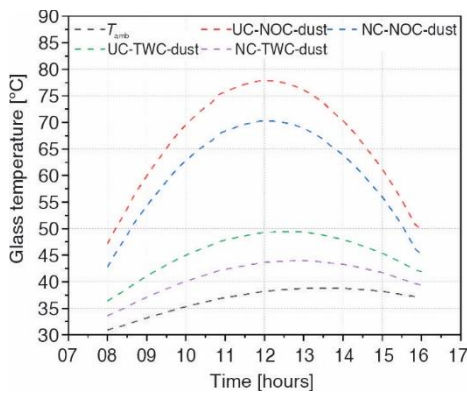


Figure 9. Glass temperature for day 40

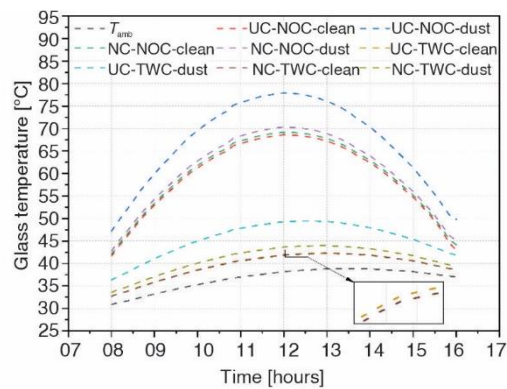


Figure 10. Comparison of glass temperature for dusted and cleaned panel on day 40

Figure 10 shows the PV module temperature for different configurations viz. UC-NOC, NC-NOC, UC-TWC and NC-TWC dusted and cleaned panel. The UC-NOC, NC-NOC, UC-TWC, and NC-TWC cleaned panels attained the maximum glass temperatures of 68.59 °C, 69.18 °C, 42.38 °C, and 42.28 °C on day 40, respectively. The average temperature rise between the dusted and cleaned panels for UC-NOC, NC-NOC, UC-TWC, and NC-TWC were 7.82 °C (13.16%), 0.96 °C (1.61%), 5.88 °C (14.76%), and 1.43 °C (3.60%), respectively. Humidity and dust particulate matter (PM 2.5 and PM 10) in the atmosphere deposit over the PV module over time. This causes some solar radiation to be absorbed and scattered on the top glass surface, raising the module's temperature.

Using graphene nanocoat over a no-cooling solar PV module can decrease the module temperature by about 6.32 °C (9.36%) compared to a UC-NOC panel. Also, the NC-TWC PV panel can decrease the module temperature by about 26.19 °C (38.20%) and 4.52 °C (9.86%) compared to UC-NOC and UC-TWC. The decrease in temperature of the nano-coated PV module indicates the effect of nanocoating minimizing the dust deposition over time, leading to a decrease in the module temperature.

Figure 11 illustrates the output power of a PV module on day 1 for various configurations, including UC-NOC, NC-NOC, UC-TWC, and NC-TWC. The results show that the maximum rated output power attained by the PV module on day 1 is 137.50 W for UC-NOC, 137.10 W for NC-NOC, 161.60 W for UC-TWC, and 161.80 W for NC-TWC. Also, the nano-coated no-cooling solar PV module can decrease the module output power by about 0.33 W (0.29%) compared to the un-coated no-cooling panel. In contrast, the NC-TWC PV panel can increase the module output power by about 15.42 W (12.63%) and 0.14 W (0.10%) compared to UC-NOC and UC-TWC. On day 1, when compared with the UC-NOC module, the NC-NOC module experienced a decrease in output power, but at the same time, the NC-TWC module increased the output power compared with the UC-TWC.

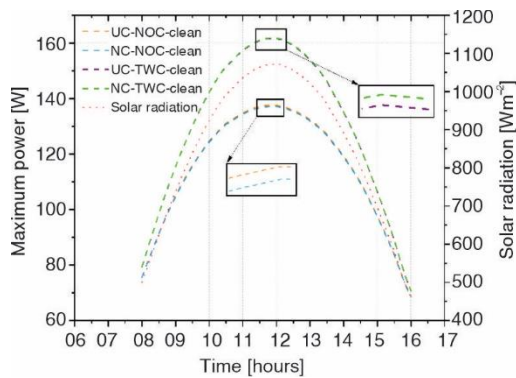


Figure 11. Maximum power for day 1

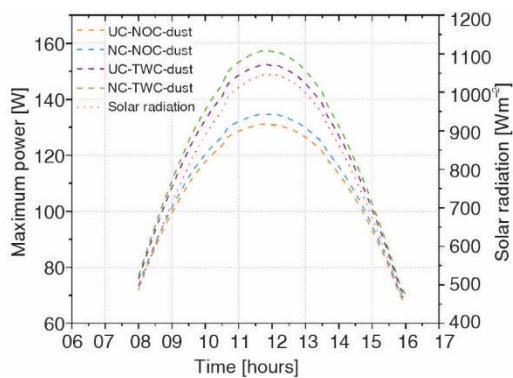


Figure 12. Maximum power for day 20

Figure 12 presents the PV module output of an experimental investigation conducted on day 20 for the various configurations of dusted module. The UC-NOC, NC-NOC, UC-TWC, and NC-TWC dusted panels attain the maximum output power of 131.10 W, 134.70 W, 152.40 W and 157.40 W on day 20, respectively. Using graphene nano-coat over a no-cooling solar PV module can increase the module output power by about 2.52 W (2.22%) compared to a UC-NOC panel. Also, the NC-TWC PV panel can increase the module output power by about 16.75 W (14.44%) and 3.32 W (2.58%) compared to UC-NOC and UC-TWC. Furthermore, Nano-

coating over a PV module surface has a positive impact on the cooling of the solar PV module and increases the panel output power beyond day 1 for the NC-NOC PV module.

Figure 13 presents the PV module output power of an experimental investigation conducted on day 40 for the various configurations of the dusted module. The UC-NOC, NC-NOC, UC-TWC, and NC-TWC dusted panels attain the maximum output power of 127.50 W, 134.20 W, 151.0 W and 157.0 W on day 40, respectively. Figure 14 shows the PV Module output power for different configurations viz. UC-NOC, NC-NOC, UC-TWC, and NC-TWC dusted and cleaned panel. The UC-NOC, NC-NOC, UC-TWC, and NC-TWC cleaned panels attained the maximum output power of 135.6 W, 135.2 W, 158.6 W, and 158.8 W on day 40, respectively. The average decrease in output power between the dusted and cleaned panels for UC-NOC, NC-NOC, UC-TWC, and NC-TWC were 5.65 W (4.82%), 0.69 W (0.59%), 5.12 W (3.82%), and 1.24 W (0.93%), respectively. Humidity and dust particulate matter (PM 2.5 and PM 10) in the atmosphere deposit over the PV module over time. Using graphene nanocoat over a no-cooling solar PV module can increase the module output power by about 4.65 W (4.16%) compared to a UC-NOC panel. Also, the NC-TWC PV panel can increase the module output power by about 19.15 W (16.87%) and 4.0 W (3.11%) compared to UC-NOC and UC-TWC. The decrease in temperature of the nano-coated PV module indicates the effect of nano-coating minimizing the dust deposition over time, leading to a increase in the module output power.

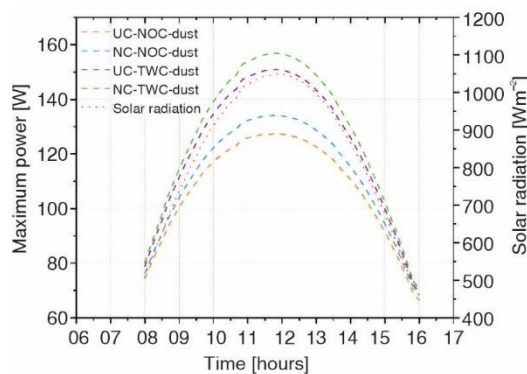


Figure 13. Maximum power for day 40

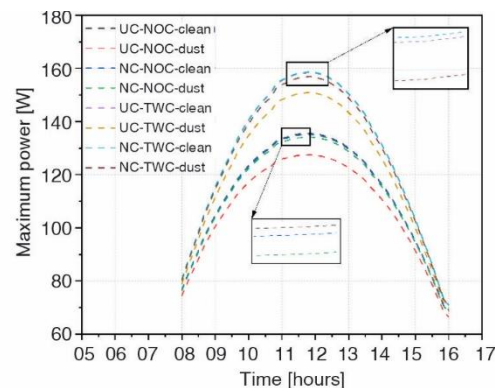


Figure 14. Comparison of maximum power for dusted and cleaned panel on day 40

Figure 15 illustrates the efficiency of a PV module on day 1 for various configurations, including UC-NOC, NC-NOC, UC-TWC, and NC-TWC. The results show that the maximum efficiency attained by the PV module on day 1 is 15.56% for UC-NOC, 15.53% for NC-NOC, 16.31% for UC-TWC, and 16.32% for NC-TWC. Also, the nanocoated no-cooling solar PV module can decrease the module efficiency by about 0.04% compared to the un-coated no-cooling panel. In contrast, the NC-TWC PV panel can increase the module efficiency by about 1.78% and 0.01% compared to UC-NOC and UC-TWC. On day 1, when compared with the UC-NOC module, the NC-NOC module experienced a decrease in efficiency, but at the same time, the NC-TWC module increased the efficiency compared with the UC-TWC.

Figure 16 presents the PV module efficiency of an experimental investigation conducted on day 20 for the various configurations of dusted module. The UC-NOC, NC-NOC, UC-TWC, and NC-TWC dusted panels attain the maximum efficiency of 15.3%, 15.5%, 16.0%, and 16.3% on day 20, respectively. Using graphene nanocoat over a no-cooling solar

PV module can increase the module efficiency by about 0.3% compared to a UC-NOC panel. Also, the NC-TWC PV panel can increase the module efficiency by about 1.95% and 0.39% compared to UC-NOC and UC-TWC. Furthermore, The nano-coating over a PV module surface has a positive impact on the cooling of the solar PV module and increases the panel efficiency beyond day 1 for the NC-NOC PV module.

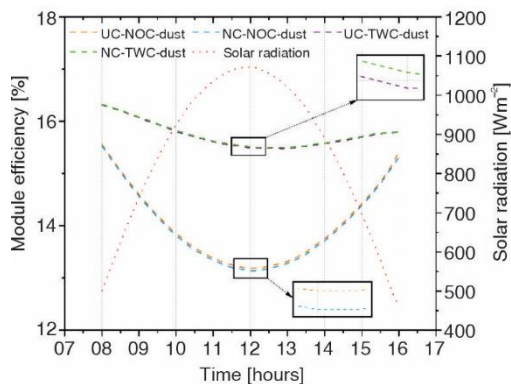


Figure 15. Module efficiency for day 1

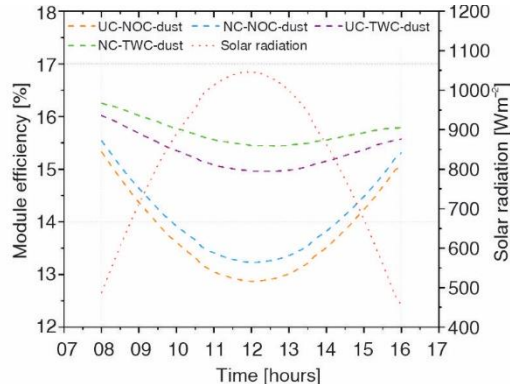


Figure 16. Module efficiency for day 20

Figure 17 presents the PV module efficiency of an experimental investigation conducted on day 40 for the various configurations of the dusted module. The UC-NOC, NC-NOC, UC-TWC, and NC-TWC dusted panels attain the maximum efficiency of 15.0%, 15.4%, 15.9%, and 16.2% on day 40, respectively. Figure 18 shows the PV module efficiency for different configurations viz. UC-NOC, NC-NOC, UC-TWC, and NC-TWC dusted and cleaned panel. The UC-NOC, NC-NOC, UC-TWC, and NC-TWC cleaned panels attained the maximum efficiency of 15.5%, 15.5%, 16.3%, and 16.3% on day 40, respectively. The average decrease in efficiency between the dusted and cleaned panels for UC-NOC, NC-NOC, UC-TWC, and NC-TWC were 0.67%, 0.08%, 0.6%, and 0.15%, respectively. Humidity and dust particulate matter (PM 2.5 and PM 10) in the atmosphere deposit over the PV module over time.

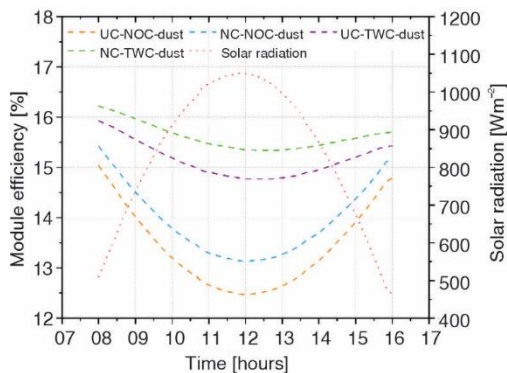


Figure 17. Module efficiency for day 40

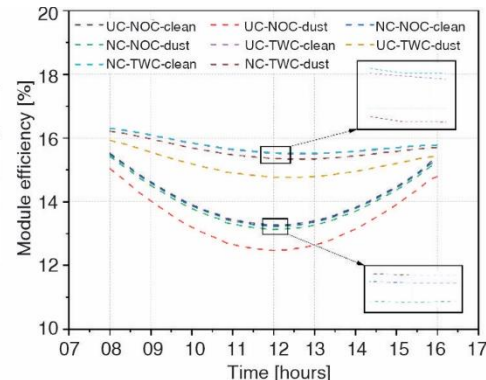


Figure 18. Comparison of Module efficiency for dusted and cleaned panel on day 40

Using graphene nanocoat over a no-cooling solar PV module can increase the module efficiency by about 0.55% (3.3%) compared to a UC-NOC panel. Also, the NC-TWC PV panel

can increase the module efficiency by about 2.22% (13.22%) and 0.47% (2.82%) compared to UC-NOC and UC-TWC. The decrease in temperature of the nano-coated PV module indicates the effect of nano-coating minimizing the dust deposition over time, leading to an increase in the module efficiency.

Conclusions

This experimental study aimed to enhance the performance of PV solar panels by reducing dust accumulation and managing module temperature using graphene hydrophobic nanocoating coupled with top water cooling. The study was conducted over 40 days with eight simultaneous experiments, monitoring PV characteristics, output power, solar radiation, ambient temperature, and efficiency. On day 1, compared to the UC-NOC module, the NC-NOC module exhibited a 0.55 °C increase in glass temperature, while the NC-TWC module showed a reduction of 20.34 °C. Over time, the nano-coating reduced the panel temperature, and on day 40, it demonstrated a 9.36% reduction compared to a dusty panel and 3.8% compared to a manually cleaned panel without coating. The graphene nanocoating on the PV module increased the output power and efficiency by 4.16% and 3.3%, respectively, compared to the UC-NOC panel. The NC-TWC panel demonstrated even more significant improvements, with a 16.87% increase in power and 13.22% increase in efficiency compared to UC-NOC, and 3.11% and 2.82% improvements compared to UC-TWC, respectively. The decrease in temperature and improved performance indicate that the nanocoating effectively minimizes dust deposition, resulting in higher module power and efficiency. The graphene hydrophobic coating serves as a protective barrier against dust, moisture, and contaminants, while the water-cooling system regulates temperature and enhances overall panel performance. Future research could focus on scaling the integration of graphene nanocoating and water cooling for large-scale solar installations. Exploring the use of different nanocoating materials to enhance efficiency and dust resistance is also recommended. Additionally, investigating the economic feasibility and environmental impact of these technologies for commercial applications would be valuable.

Nomenclature

A	– surface area [m ²]
G	– solar irradiance [Wm ⁻²]
I	– current [A]
n	– total number of variables
P	– power [W]
PM	– particulate matter [μgm ⁻³]
R	– measurement results
T	– ambient temperature [°C]
U	– overall uncertainty
V	– voltage [V]
x_i	– measured variables

Greek symbols

θ	– tilt angle
η	– efficiency

Superscripts

amb	– ambient
ele	– electrical
mp	– maximum power
oc	– open circuit
sc	– short circuit

Acronyms

MPPT	– maximum power point tracking
NC-NOC	– nano coated no cooling
NC-TWC	– nano coated top water cooling
PVC	– polyvinyl chloride
UC-NOC	– uncoated no cooling
UC-TWC	– uncoated top water cooling

References

- [1] Ilse, K., *et al.*, Advanced Performance Testing of Anti-Soiling Coatings-Part II: Particle-Size Dependent Analysis for Physical Understanding of Dust Removal Processes and Determination of Adhesion Forces, *Solar Energy Materials and Solar Cells*, 202 (2019), 110049

- [2] Piliouguine, M., *et al.*, Comparative Analysis of Energy Produced by Photovoltaic Modules with Anti-Soiling Coated Surface in Arid Climates, *Applied Energy*, 112 (2013), Dec., pp. 626-634
- [3] Zhang, L., *et al.*, Indoor Experiments of Dust Deposition Reduction on Solar Cell Covering Glass by Transparent Super-Hydrophobic Coating with Different Tilt Angles, *Solar energy*, 188 (2019), Aug., pp. 1146-1155
- [4] Mozumder, M. S., *et al.*, Recent Developments in Multifunctional Coatings for Solar Panel Applications: A Review, *Solar Energy Materials and Solar Cells*, 189 (2019), Jan., pp. 75-102
- [5] Abdo, S., Hind, S., Effect of Using Saturated Hydrogel Beads with Alumina Water-Based Nanofluid for Cooling Solar Panels: Experimental Study with Economic Analysis, *Solar Energy*, 217 (2021), Mar., pp. 155-164
- [6] Almuwailhi, A., Zeitoun, O., Investigating the Cooling of Solar Photovoltaic Modules Under the Conditions of Riyadh, *Journal of King Saud University-Engineering Sciences*, 35 (2023), 2, pp. 123-136
- [7] Sethiya, A., Cooling Material for Solar PV Module to Improve the Generation Efficiency, *Materials Today: Proceedings*, 47 (2021), Part 19, pp. 7064-7066
- [8] Elbreki, A. M., *et al.*, Experimental and Economic Analysis of Passive Cooling PV Module Using Fins and Planar Reflector, *Case Studies in Thermal Engineering*, 23 (2021), 100801
- [9] Al-Amri, F., *et al.*, Innovative Technique for Achieving Uniform Temperatures Across Solar Panels Using Heat Pipes and Liquid Immersion Cooling in the Harsh Climate in the Kingdom of Saudi Arabia, *Alexandria Engineering Journal*, 61 (2022), 2, pp. 1413-1424
- [10] Sharma, V., Shyam S. C., Performance and Degradation Analysis for Long Term Reliability of Solar Photovoltaic Systems: A Review, *Renewable and Sustainable Energy Reviews*, 27 (2013), Nov., pp. 753-767
- [11] He, G., *et al.*, Review of Self-Cleaning Method for Solar Cell Array, *Procedia Engineering*, 16 (2011), Dec., pp. 640-645
- [12] Moghimi, M. A., Ahmadi, G., Wind Barriers Optimization for Minimizing Collector Mirror Soiling in a Parabolic Trough Collector Plant, *Applied Energy*, 225 (2018), Sept., pp. 413-423
- [13] Elnozahy, A., *et al.*, Efficient energy Harvesting from PV Panel with Reinforced Hydrophilic Nano-Materials for Eco-Buildings, *Energy and Built Environment*, 5 (2024), 3, pp. 393-403
- [14] Zhang, R., *et al.*, High Performance Photovoltaic/Thermal Subsystem Photoelectric Conversion Solar Cell Coupled Thermal Energy Storage System, *Thermal Science*, 24 (2020), 5B, pp. 3213-3220
- [15] Fares, E., Yusuf, B., Comparative Performance Evaluation of c-Si and GaAs Type PV Cells with and without Anti-Soiling Coating Using Energy and Exergy Analysis, *Renewable energy*, 146 (2020), Feb., pp. 1010-1020
- [16] Vedula, G., Geetha, A., Dust Accumulation on Solar Photovoltaic Panels: An Investigation Study on Power Loss and Efficiency Reduction, *Thermal Science*, 27 (2023), 4A, pp. 2967-2976
- [17] Bazzari, H. H., *et al.*, Cooling Solar Cells Using ZnO Nanoparticles as a Down-Shifter, *Thermal Science*, 24 (2020), 2A, pp. 809-814
- [18] Zhang, L., *et al.*, Indoor Experiments of Dust Deposition Reduction on Solar Cell Covering Glass by Transparent Super-Hydrophobic Coating with Different Tilt Angles, *Solar energy*, 188 (2019), Aug., pp. 1146-1155
- [19] Jaszczur, M., *et al.*, Impact of Dust and Temperature on Energy Conversion Process in Photovoltaic Module, *Thermal Science*, 23 (2019), 4, pp. 1199-1210
- [20] ***, BT Corp Generic Nano Private Ltd., <https://www.bt-corp.co>
- [21] Holman, J. P., *Experimental Methods for Engineers*, McGraw-Hill Education, New York, USA, 2012
- [22] ***, India Meteorological Department Government of India, <https://mausam.imd.gov.in>